

# UniFusion: A Unified Image Fusion Framework with Robust Representation and Source-Aware Preservation

Xingyuan Li<sup>1\*</sup>, Songcheng Du<sup>2\*</sup>, Yang Zou<sup>2</sup>, HaoYuan Xu<sup>3</sup>, Zhiying Jiang<sup>4†</sup>, Jinyuan Liu<sup>3</sup>

<sup>1</sup> Zhejiang University, <sup>2</sup> Northwest Polytechnical University,

<sup>3</sup> Dalian University of Technology, <sup>4</sup> Dalian Maritime University

xingyuan\_lxy@163.com, dusongcheng@mail.nwpu.edu.cn

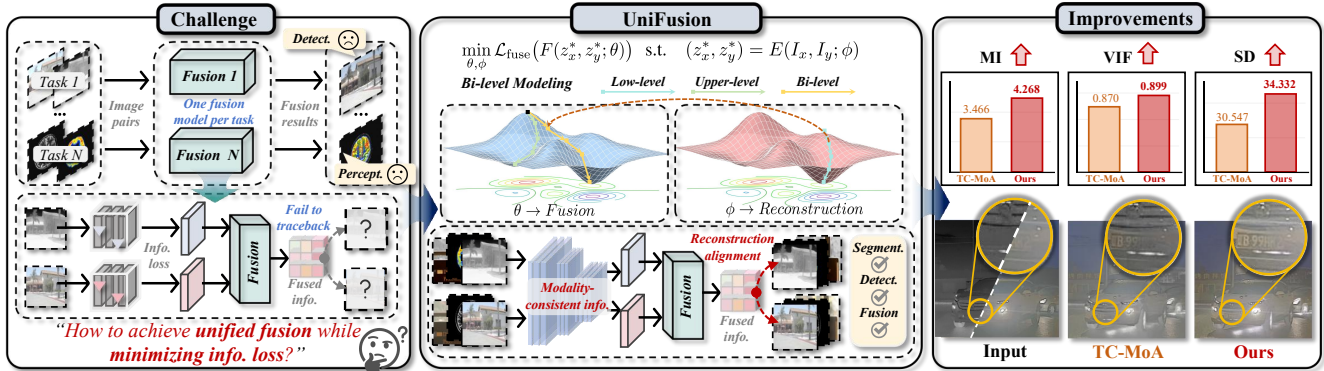


Figure 1. Overview of the proposed bilevel optimization framework for unified image fusion task. **(Left)** Conventional approaches are typically designed for task-specific scenarios and struggle to effectively preserve source information during the fusion process, leading to inconsistent modality representation and information loss. **(Middle)** Our UniFusion formulates fusion as a bilevel optimization problem. The lower-level reconstruction branch learns modality-consistent representations through self-reconstruction, while the upper-level fusion branch adaptively integrates them into a unified representation that effectively enhances semantic preservation and structural integrity. **(Right)** Quantitative and qualitative results demonstrate that our method consistently outperforms TC-MoA across multiple metrics.

## Abstract

Image fusion aims to integrate complementary information from multiple source images to produce a more informative and visually consistent representation, benefiting both human perception and downstream vision tasks. Despite recent progress, most existing fusion methods are designed for specific tasks (i.e., multi-modal, multi-exposure, or multi-focus fusion) and struggle to effectively preserve source information during the fusion process. This limitation primarily arises from task-specific architectures and the degradation of source information caused by deep-layer propagation. To overcome these issues, we propose **UniFusion**, a unified image fusion framework designed to achieve cross-task generalization. First, leveraging DINOv3 for modality-consistent feature extraction, UniFusion establishes a shared semantic space for diverse inputs. Second, to preserve the understanding of each

source image, we introduce a reconstruction-alignment loss to maintain consistency between fused outputs and inputs. Finally, we employ a bilevel optimization strategy to decouple and jointly optimize reconstruction and fusion objectives, effectively balancing their coupling relationship and ensuring smooth convergence. Extensive experiments across multiple fusion tasks demonstrate UniFusion’s superior visual quality, generalization ability, and adaptability to real-world scenarios. Code is available at <https://github.com/dusongcheng/UniFusion>.

## 1. Introduction

Image fusion seeks to integrate complementary information from multiple source images into a single, informative, and visually coherent representation [64, 71]. As a fundamental problem in computer vision, it plays a critical role in enhancing scene understanding, facilitating robust decision-making, and supporting downstream tasks such as object detection [31], medical diagnosis [14], autonomous navigation [29], and low-light surveillance [57].

\*These authors contributed equally.

†Corresponding author.

Driven by the rapid progress in deep learning, image fusion has undergone remarkable advances in recent years [56, 63, 66]. Most methods are primarily designed for specific fusion scenarios, including Infrared and Visible Image Fusion (IVIF) [30, 61, 62], multi-exposure fusion [11, 39], multi-focus fusion [1, 50], and medical image fusion [26, 40]. These methods employ customized designs and utilize diverse architectures such as CNNs [21], autoencoders, and GANs to extract features for image fusion [37]. However, these task-specific methods have limited generalization capabilities and struggle to adapt to diverse fusion requirements, prompting researchers to explore general fusion frameworks.

To adapt to diverse tasks, recent general image fusion methods aim to handle multiple heterogeneous inputs and fusion tasks with a single model, exhibiting diverse development trends in recent years. Transformer-based architectures [34, 64] leverage self-attention mechanisms to model global dependencies across modalities and process different types of image pairs through unified feature interaction modules [32]; diffusion model-based methods [13, 65] iteratively denoise to generate high-quality fusion results through universal data distributions; other methods [51, 57] construct unified representation spaces by designing task-agnostic fusion modules and shared feature extractors.

Although these methods have achieved significant breakthroughs in fusion quality and semantic understanding, the generalization capabilities of existing general fusion systems remain limited. These approaches generally employ shared backbones and task-agnostic fusion modules to build a common representation space. While promising, their generalization capability is still constrained by two key factors: (1) the lack of a principled, modality-consistent feature extraction mechanism that can robustly encode heterogeneous signals under diverse conditions, and (2) the difficulty in preserving critical information from each source image during deep feature propagation, which leads to information degradation and sub-optimal fusion quality across tasks.

To address these limitations, we propose UniFusion, a robust and unified image fusion framework that enhances the understanding and preservation of source information while achieving superior cross-task generalization. First, we incorporate the powerful self-supervised visual representation capability of DINOv3 [44] to construct a generalizable feature extraction backbone, enabling modality-consistent and robust feature learning across diverse image types. Second, we introduce a reconstruction-alignment mechanism that leverages intermediate features to reconstruct source images, enforcing strong information retention and ensuring faithful semantic alignment during fusion. Finally, we formulate fusion and reconstruction as a bilevel optimization problem, decoupling and jointly optimizing the two objectives to achieve an improved balance between

information preservation and fusion quality. Comprehensive experiments across multi-modal, multi-exposure, and multi-focus tasks validate the effectiveness and generalization ability of UniFusion. Our main contributions are summarized as follows:

- A unified fusion architecture with strong cross-task generalization. We present a universal fusion framework that effectively addresses the generalization limitations of existing fusion models.
- Modality consistent feature extraction and reconstruction aligned fusion. We design a universal feature extractor based on DINOv3 and introduce a reconstruction-alignment mechanism that enforces consistent understanding and preservation of source information.
- Bilevel optimization for balanced fusion and source fidelity. We formulate fusion and reconstruction as a bilevel optimization problem, achieving superior fusion performance while better retaining structural, semantic, and modality-specific information from source images.

## 2. Related work

### 2.1. Task-specific Image Fusion Methods

Image fusion is a fundamental enhancement technique and a long-standing research focus [35, 70]. Within this field, mainstream schemes, particularly task-specific ones, can be classified into the following categories.

**Infrared-visible Image Fusion:** This task aims to integrate thermal information from infrared images [24] with texture details from visible images [19]. Early deep learning approaches include supervised convolutional neural networks [28]. To mitigate misalignment, generation-registration-fusion pipelines [47] and spatial-frequency integration networks [3, 68] have been developed.

**Medical Image Fusion:** This task focuses on preserving distinct tissue characteristics from multi-modal medical data (e.g., CT/MRI) to support clinical diagnosis, with a focus on content-aware feature preservation [8, 15]. Das et al. proposed a content-aware GAN [2] for this purpose. Tang et al. developed FATFusion [45], a dual-branch Transformer framework that explicitly models the distinct properties of functional and anatomical modalities.

**Multi-exposure Image Fusion:** This task focuses on synthesizing a high-dynamic-range image from a sequence of captures of the same scene under varying exposures [6, 23]. The core challenge lies in achieving balanced brightness and preserving fine details. Xu et al. proposed MEF-GAN [53], and Zhang et al. further optimized this with MFF-GAN [58]. Ouyang et al. [39] combine GCNs and lightweight CNNs for real-time applications.

## 2.2. General Image Fusion Methods

While task-specific methods demonstrate strong performance within their domains by leveraging specialized priors, they often operate in isolation, overlooking the potential synergies and common underlying principles across different fusion tasks. This limitation has motivated the development of unified frameworks that aim to capture these inherent associations.

**Advanced Architecture-based Methods:** This line of research focuses on building unified frameworks by leveraging the complementary strengths of CNNs and Transformers [5, 67]. Liu et al. proposed CSR [33] using a convolutional sparse representation. Subsequently, U2Fusion pioneered an all-in-one approach [51]. Ma et al. developed SwinFusion [34], a cross-domain Swin Transformer framework. Duan et al. designed a hybrid CNN-Transformer architecture [4] with online knowledge distillation.

**Large Model and Emerging Paradigm-based Methods:** Recent trends explore integrating capabilities from large models [17, 25, 36, 49], such as text guidance [22, 42, 54], diffusion models [48], and adapter modules [43], to enhance semantic awareness and handle cross-task disparities. Building upon these advances, Yi et al. introduced TextIF [57], a text-guided framework. Zhu et al. proposed TC-MoA [69], which uses a task-specific routing network to unify multiple fusion tasks.

## 3. Method

### 3.1. Overview

We propose a unified image fusion framework that leverages the semantic representation capability of DINOv3 to achieve modality-consistent and generalizable feature integration. As illustrated in Fig. 2, two frozen DINOv3 backbones are employed to extract semantically rich features from each modality, while lightweight adapters are introduced to modulate domain-specific characteristics and reduce distributional discrepancies. The adapted features are then fused through several cross-attention modules that dynamically model inter-modality dependencies and emphasize complementary information. To avoid information loss and semantic drift, each adapter is paired with a reconstruction branch that decodes its adapted embedding back to the original input and is supervised independently. Finally, the entire framework is jointly optimized under a hybrid objective that balances semantic alignment, reconstruction fidelity, and fusion consistency, ensuring both effective information preservation and semantic-level integration across diverse fusion scenarios.

### 3.2. Semantic Prior Adaptation with DINOv3

To achieve modality-consistent and generalizable feature representation, we employ DINOv3, a self-supervised Vi-

sion Transformer pretrained on large-scale natural images, as the universal semantic backbone. Unlike conventional modality-specific encoders that are prone to overfitting and fail to generalize across domains, DINOv3 offers object-centric priors and long-range contextual dependencies, which provide a strong foundation for cross-modal representation learning. Given an input image  $I_m \in \mathbb{R}^{H \times W \times 3}$  from modality  $m$ , the image is first divided into non-overlapping patches and linearly projected into  $d$ -dimensional token embeddings. These tokens are propagated through  $L$  transformer layers of the frozen DINOv3 encoder, from which a subset of intermediate feature maps is extracted to form a semantic hierarchy that jointly encodes local structural cues and global contextual semantics.

Despite its strong generalization, DINOv3 is pretrained on large-scale natural images, and its latent space may not perfectly align with modality-specific characteristics. To address this domain discrepancy, we introduce a lightweight, hierarchical Adapter that performs progressive feature recalibration across multiple semantic scales.

Conceptually, the Adapter functions as a progressive feature translator, refining multi-level ViT representations into modality-aligned embeddings. It employs a cascade of multi-stage fusion and upsampling operations, in which transformer features extracted from multiple layers ( $f^{(l_2)}$ ,  $f^{(l_5)}$ ,  $f^{(l_8)}$ ,  $f^{(l_{11})}$ ) are sequentially integrated through a residual hierarchy. Each fusion stage aggregates global semantic cues from deeper layers with fine-grained structural details from shallower ones, enabling a smooth semantic–structural transition across scales. This hierarchical integration not only enhances representational fidelity but also enforces distributional consistency across modalities, providing a robust and unified feature space for subsequent fusion and reconstruction.

### 3.3. Reconstruction Alignment

Although the proposed dual-branch architecture effectively adapts pretrained DINOv3 representations to diverse modalities, direct fusion of such embeddings may still suffer from semantic drift and information loss. As features from heterogeneous sources are projected into a shared latent space, modality-specific cues, such as texture in visible images or radiometric contrast in infrared ones, tend to weaken, leading to suboptimal alignment and degraded reconstruction fidelity.

Existing image fusion methods predominantly emphasize the similarity between the fused output and the source images, often adopting pixel-level or appearance-based supervision to preserve visual details. However, such low-level constraints tend to bias the model toward reproducing superficial texture or intensity patterns, rather than capturing deeper semantic correspondences across modalities. Consequently, these often overfit to appearance details

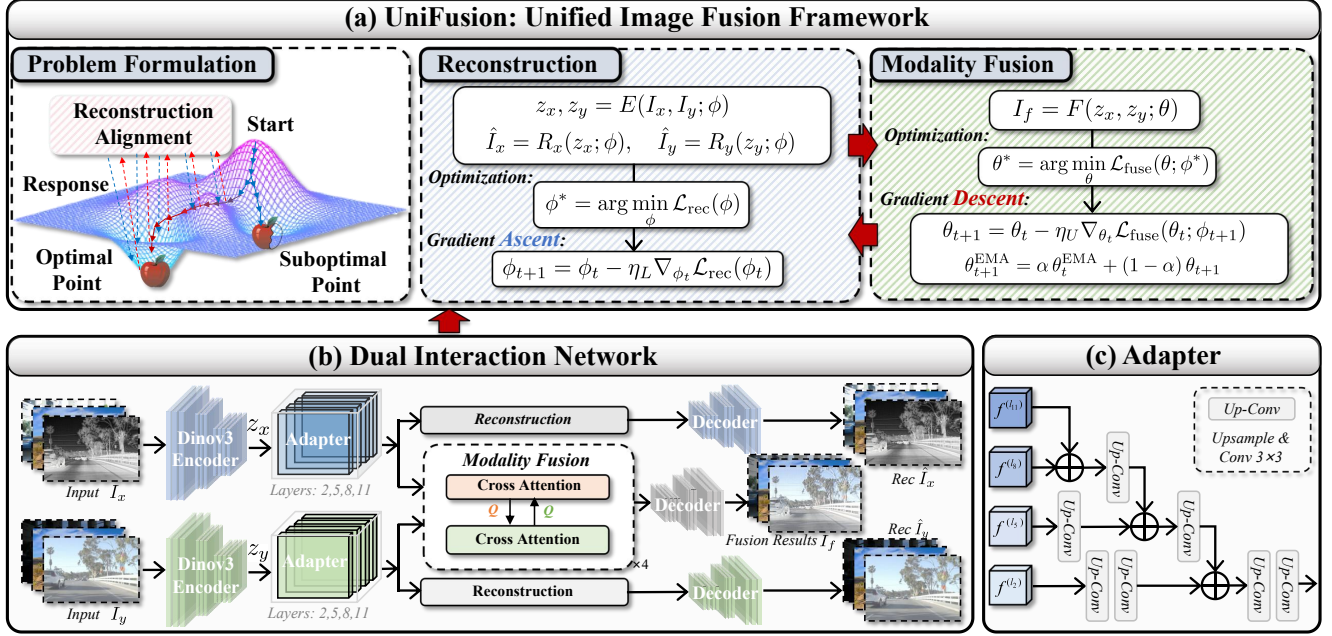


Figure 2. Overview of the proposed UniFusion framework.

while failing to maintain high-level consistency.

To mitigate this issue, we introduce a reconstruction-alignment mechanism that explicitly regularizes the fusion process through self-reconstruction constraints. The core idea is to ensure that the encoded latent representation retains sufficient modality-specific information to reconstruct the original inputs, thereby enforcing semantic fidelity and preventing information loss.

Concretely, for each modality  $m$ , the adapter produces a calibrated feature map  $\hat{\mathbf{F}}_m$ , which is passed through a lightweight reconstruction branch composed of a few Transformer layers and a projection head:

$$\bar{I}_m = R_m(\hat{\mathbf{F}}_m) \quad (1)$$

where  $R_m(\cdot)$  denotes the reconstruction function.

### 3.4. Bilevel Optimization

To jointly optimize semantic reconstruction and modality fusion operating at different temporal dynamics, we formulate the learning process as a bilevel optimization problem. In this hierarchical formulation, the inner loop rapidly updates reconstruction-oriented representations to capture modality-specific semantics, while the outer loop gradually adjusts the fusion strategy based on the evolving feature space. This two-layer interaction facilitates stable co-adaptation between feature encoding and fusion, ultimately achieving a balanced tradeoff between semantic consistency and structural fidelity in the final fused result.

Formally, let  $\phi$  denote the parameters of the adapter and reconstruction subnetworks responsible for modality-

specific representation, and  $\theta$  represent the parameters of the fusion network. Given an image pair  $(I_x, I_y)$ , the feature encoding and reconstruction processes can be expressed as:

$$z_x, z_y = E(I_x, I_y; \phi), \quad \hat{I}_x = R_x(z_x; \phi), \quad \hat{I}_y = R_y(z_y; \phi), \quad (2)$$

while the fusion result is obtained by:

$$I_f = F(z_x, z_y; \theta). \quad (3)$$

The overall training objective is then formulated as a bilevel optimization problem:

$$\phi^* = \arg \min_{\phi} \mathcal{L}_{\text{rec}}(\phi), \theta^* = \arg \min_{\theta} \mathcal{L}_{\text{fuse}}(\theta; \phi^*) \quad (4)$$

The inner-level objective focuses on reconstructing each modality to preserve semantic and structural fidelity, guiding the encoders to produce features that are rich in modality-aware cues. The outer-level objective then learns an optimal fusion strategy based on these representations, ensuring complementary information is integrated effectively.

In practice, directly solving this nested optimization is computationally expensive. Therefore, we employ a first-order alternating scheme, where the two parameter sets are updated sequentially within each iteration:

$$\begin{aligned} \phi_{t+1} &= \phi_t - \eta_L \nabla_{\phi_t} \mathcal{L}_{\text{rec}}(\phi_t), \\ \theta_{t+1} &= \theta_t - \eta_U \nabla_{\theta_t} \mathcal{L}_{\text{fuse}}(\theta_t; \phi_{t+1}), \end{aligned} \quad (5)$$

where  $\eta_L$  and  $\eta_U$  denote the learning rates for the inner and outer levels, respectively, typically satisfying  $\eta_L > \eta_U$  to ensure faster representation adaptation.

To further enhance the temporal stability of the fusion dynamics, we introduce an exponential moving average (EMA) regularization on the outer parameters:

$$\theta_{t+1}^{\text{EMA}} = \alpha \theta_t^{\text{EMA}} + (1 - \alpha) \theta_{t+1}, \quad (6)$$

where  $\alpha \in [0, 1)$  controls the momentum of the update.

## 4. Experiment

### 4.1. Experimental Setting

**Dataset.** We evaluate the proposed framework across four representative image fusion tasks, including infrared–visible image fusion (IVIF), medical image fusion (MIF), multi-exposure image fusion (MEF), and multi-focus image fusion (MFF). For IVIF, experiments are conducted on three widely adopted benchmark datasets: M3FD [28], TNO [46], and RoadScene [52], which collectively cover diverse illumination, object, and background conditions. For MIF tasks, we employ the Medical Harvard dataset<sup>3</sup>. The MEF and MFF tasks are evaluated using the MEFB [59] and MFIF [60] benchmarks, respectively. The MFIF collection integrates multiple sub-datasets, including Lytro [38], MFFW [55], and MFI-WHU [58], offering a comprehensive evaluation of multi-focus fusion under varied scene configurations.

**Implementation Details.** Our experiments are performed on an NVIDIA RTX 5090 GPU. The batch size is set to 16, and each fusion task is trained for 10,000 iterations. During training, images are randomly cropped into 128×128 patches and normalized to the range [0,1] [20, 41]. Model parameters are optimized using the Adam optimizer, with the learning rate initialized to  $2 \times 10^{-4}$  and decayed exponentially during training [7, 10]. The fusion network consists of four Cross-Attention Blocks, while each reconstruction branch includes four Transformer Blocks. The fusion optimization follows the loss formulation of SwinFusion [34], ensuring fair comparison and stable convergence across different fusion tasks. In addition, we incorporate a reconstruction loss in a self-supervised manner, where each source image is reconstructed from the fused representation using an L1 loss.

**Benchmarks.** We compare our method against ten recent state-of-the-art image fusion approaches, including CDDFuse [64], CoCoNet [31], DeFuse [27], LRR-Net [18], MGDN [9], ReCoNet [12], SwinFusion [34], U2Fusion [51], UMFusion [47], and TC-MoA [69].

### 4.2. Evaluation on Multi-Modal Image Fusion

**Quantitative Comparisons.** We quantitatively evaluate the fusion performance using four widely adopted metrics: Mutual Information (MI), Visual Information Fidelity (VIF),

$Q_{abf}$  and  $Q_y$ , as shown in Tab. 1. Our method consistently outperforms existing general-purpose fusion algorithms across multiple infrared–visible fusion benchmarks, demonstrating strong generalizability and modality compatibility. Notably, the improvements in VIF,  $Q_{abf}$  and  $Q_y$ , which are closely related to human visual perception and information preservation, indicate that the fused images generated by our framework retain richer structural and semantic details from the source inputs. In addition, the higher MI value further confirms that our method effectively maintains both mutual information characteristics, leading to more perceptually faithful and information-rich fusion results.

**Qualitative Comparisons.** As illustrated in Fig. 4, our method exhibits superior visual performance compared with other approaches. For qualitative analysis, we selected two representative samples from the M3FD and RoadScene datasets, covering diverse scenarios to ensure a comprehensive evaluation. The proposed method more effectively preserves fine texture details from the original images, such as the textures of building windows and the intricate structures at the ends of tree branches, whereas other methods tend to blur these features. Moreover, our approach highlights human contours more clearly and better maintains the mutual information between visible and infrared images. These results demonstrate the clear advantages of our method in terms of qualitative performance.

Additional results on downstream perception tasks, including object detection and semantic segmentation [16], are provided in the Appendix to further validate the effectiveness of our fusion method.

### 4.3. Evaluation on Medical Image Fusion

**Quantitative Comparisons.** We conduct quantitative experiments on the MIF dataset using five standard metrics, as illustrated in Fig. 3. The results visualize the distribution of all test samples, along with their mean and median values, revealing stable improvements across most indicators. The consistently high median scores indicate that our method maintains reliable fusion quality across diverse clinical cases, validating its robustness and effectiveness in preserving complementary modality information.

**Qualitative Comparisons.** The visual comparisons of PET–MRI fusion results are presented in Fig. 5. Competing methods often blur anatomical structures or lose soft-tissue details when PET lacks functional content, reflecting insufficient semantic alignment. In contrast, our method preserves the rich structural information from MRI while accurately integrating PET functional cues. This benefit arises from the DINOv3-guided semantic priors and hierarchical adapter design, which enable precise cross-modality calibration. Consequently, the fused images achieve both structural clarity and functional expressiveness, supporting more reliable medical interpretation.

<sup>3</sup><http://www.med.harvard.edu/AANLIB/home.html>

Dataset	M <sup>3</sup> FD Dataset				T&R Dataset				MEFB Dataset			
Method	MI $\uparrow$	VIF $\uparrow$	$Q_{abf}$ $\uparrow$	$Q_y$ $\uparrow$	MI $\uparrow$	VIF $\uparrow$	$Q_{abf}$ $\uparrow$	$Q_y$ $\uparrow$	MI $\uparrow$	VIF $\uparrow$	CC $\uparrow$	PSNR $\uparrow$
CDDFuse[64]	<u>3.776</u>	0.839	0.610	0.978	3.102	0.732	0.489	0.945	<u>6.575</u>	1.430	0.837	56.809
CoCoNet [31]	2.621	0.721	0.378	0.826	2.576	0.602	0.362	0.781	4.607	1.091	0.858	58.007
DeFuse [27]	2.924	0.612	0.332	0.959	2.991	0.667	0.393	<u>0.968</u>	5.238	1.164	0.813	58.209
LRRNet [18]	2.763	0.629	0.495	0.950	2.766	0.577	0.352	0.781	5.946	1.110	0.885	58.970
MGDN [9]	2.832	0.750	0.618	0.961	2.810	0.701	0.552	<u>0.968</u>	4.935	1.148	0.838	58.516
ReCoNet [12]	3.009	0.682	0.485	0.937	2.972	0.624	0.375	0.958	5.583	1.074	0.854	57.700
SwinFusion [34]	2.945	0.618	0.480	0.936	<u>3.325</u>	0.747	0.467	0.974	5.318	<u>1.459</u>	0.894	59.009
U2Fusion [51]	2.723	0.688	0.535	0.860	2.592	0.660	0.488	0.918	5.809	1.284	<u>0.902</u>	58.890
UMFusion [47]	3.099	0.675	0.399	0.861	2.893	0.711	0.470	0.937	6.326	1.293	0.889	58.881
TC-MoA [69]	3.466	<u>0.870</u>	<u>0.636</u>	<b>0.983</b>	3.038	<u>0.787</u>	<u>0.558</u>	0.962	4.889	1.406	0.885	<u>59.152</u>
Ours	<b>4.268</b>	<b>0.899</b>	<b>0.637</b>	<u>0.982</u>	<b>3.599</b>	<b>0.805</b>	<b>0.565</b>	<b>0.980</b>	<b>6.861</b>	<b>1.484</b>	<b>0.906</b>	<b>59.219</b>

Table 1. Quantitative comparison on M<sup>3</sup>FD, TNO, RoadScene, and MEFB datasets. The best and second best results are highlighted in **bold** and underline.

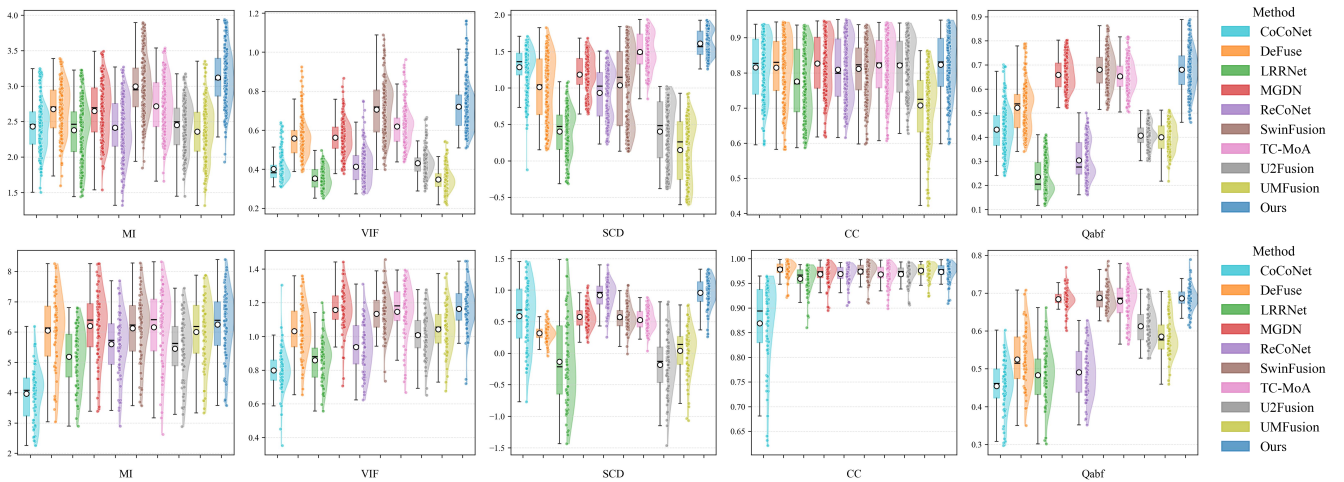


Figure 3. Quantitative comparison on MIF (top) and MFIF (bottom) datasets. The plots illustrate the distribution of all test samples across five evaluation metrics, where “-” and “o” indicate the median and mean values, respectively.

#### 4.4. Evaluation on Multi-Exposure Fusion

**Quantitative Comparisons.** We quantitatively evaluate the multi-exposure image fusion performance using four widely adopted metrics: Mutual Information (MI), Visual Information Fidelity (VIF), CC, and PSNR, as shown in Tab. 1. Our model achieves the SOTA results among general image fusion approaches, consistently outperforming competing models across most metrics. In particular, the substantial improvement in MI and VIF scores highlights the strong task adaptability of UniFusion, which effectively reconciles task-specific objectives while mitigating potential conflicts between them. Moreover, the higher CC and PSNR scores demonstrate that our method preserves structural fidelity, fine-grained textures, and overall perceptual quality more effectively.

**Qualitative Comparisons.** As illustrated in Fig. 6, our

method consistently produces visually superior fusion results compared with existing SOTA approaches. It preserves fine texture details and maintains accurate color consistency across varying illumination levels, resulting in clearer and more balanced fused images. These results further substantiate the advantages of our method in producing visually coherent and information-rich outputs.

#### 4.5. Evaluation on Multi-Focus Fusion

**Quantitative Comparisons.** We further assess UniFusion on the MFIF dataset to test its generalization to the multi-focus fusion (MFF) task. As shown in Fig. 3, our method consistently ranks among the top two across all five metrics, even without task-specific fine-tuning. This demonstrates its strong adaptability to unseen domains and effectiveness in preserving salient details across multiple focal depths.

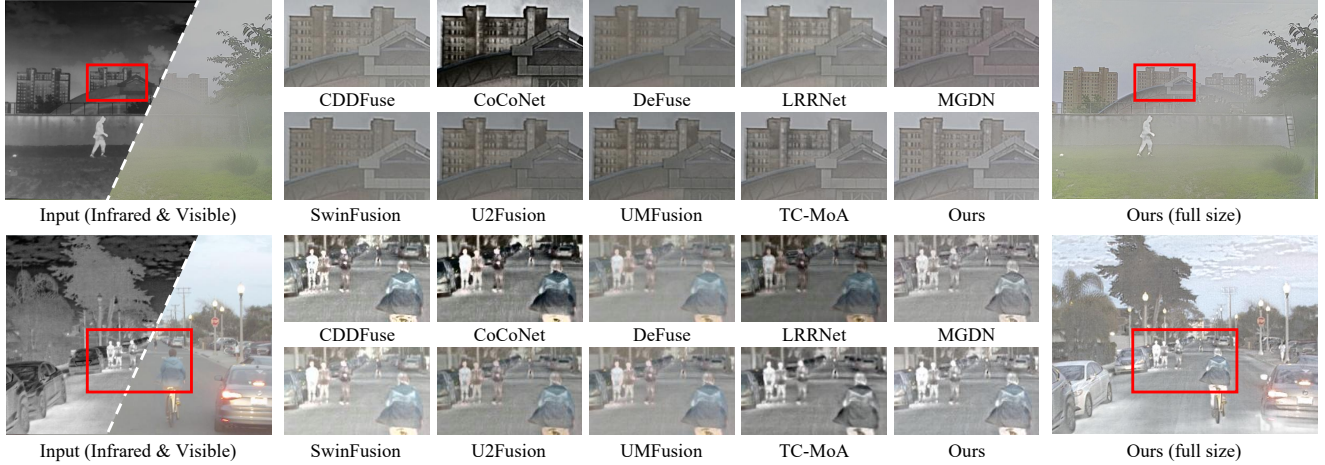


Figure 4. Visual comparison of infrared and visual image fusion results with SOTA methods on M<sup>3</sup>FD (top) and T&R (bottom) datasets.

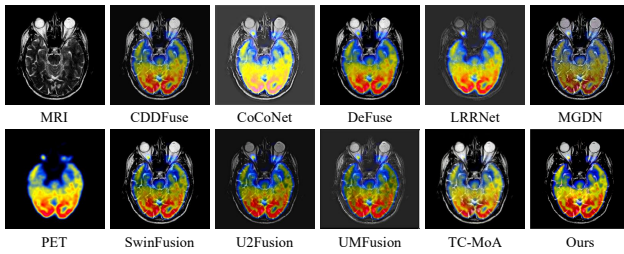


Figure 5. Visual comparison of medical image fusion results with SOTA methods on MIF dataset.

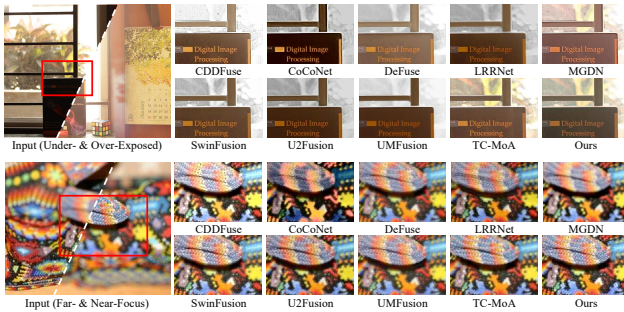


Figure 6. Visual comparison of multi-exposure image fusion and multi-focus image fusion results with SOTA methods on MEFB and MFIF datasets.

**Qualitative Comparisons.** Representative examples from the MFIF dataset are shown in Fig. 6. Our results exhibit sharper transitions and more consistent focus across regions, retaining fine textures in both near- and far-focus areas. In contrast, TC-MoA shows blur in distant regions, while LRRNet distorts near-focus details. These results highlight the superior perceptual quality and balanced fusion achieved by our method.

#### 4.6. Ablation Study

To evaluate the effectiveness and necessity of each core component in the proposed framework, we conducted a series of ablation experiments on three representative datasets, namely M3FD, MEFB, and MFIF. As summarized in Tab. 2, we designed four carefully constructed model variants to isolate and assess the contributions of key modules and training strategies. In addition, we further provide qualitative visualizations of representative samples to intuitively illustrate the influence of each module on fusion quality. As shown in Fig. 7, the full model produces clearer structural details, richer textures, and more natural visual effects compared to the ablated variants, confirming the effectiveness of the proposed components in enhancing both perceptual fidelity and information preservation.

**w/o Adapter.** In this variant, the two modality-specific adapters were removed and replaced with simple up-sampling operations for feature alignment. Without the adapter’s ability to dynamically modulate modality-specific information, the model struggled to balance two input modality representations. This resulted in a noticeable decline in overall fusion quality, particularly in measures related to information preservation and perceptual consistency. The results suggest that the adapter serves as an essential bridge between heterogeneous modalities, facilitating more coherent spatial feature integration.

**w/o DINOv3 Encoder.** To examine the role of the pre-trained semantic encoder, the DINOv3 encoder was replaced with a standard four-layer Transformer encoder. A clear degradation was observed across all datasets, especially in metrics reflecting semantic fidelity and perceptual sharpness (e.g., MI, VIF, and  $Q_{abf}$ ). These results indicate that the DINOv3 encoder introduces rich high-level semantic priors, which guide the model in aligning features from different modalities and improving the overall perceptual



Figure 7. Visual comparison of fusion results for different ablation variants on representative samples from the M<sup>3</sup>FD dataset.

Dataset	M <sup>3</sup> FD Dataset				MEFB Dataset				MFIF Dataset			
	MI↑	VIF↑	$Q_{abf}$ ↑	$Q_y$ ↑	MI↑	VIF↑	CC↑	PSNR↑	MI↑	VIF↑	CC↑	$Q_{abf}$ ↑
w/o Adapter	3.646	0.863	0.520	0.911	5.512	1.232	0.489	57.934	5.375	0.969	0.959	0.532
w/o DINOv3 encoder	3.681	0.879	0.602	0.946	5.709	1.334	0.362	58.537	5.624	0.901	0.947	0.491
w/o Reconstruction	3.846	0.870	0.587	0.932	6.434	1.396	0.393	58.779	5.838	1.013	0.961	0.579
w/o Bilevel Optimization	3.924	0.876	0.621	0.959	6.374	1.424	0.393	58.960	6.021	1.032	0.964	0.583
<b>Ours</b>	<b>4.268</b>	<b>0.899</b>	<b>0.637</b>	<b>0.982</b>	<b>6.861</b>	<b>1.484</b>	<b>0.906</b>	<b>59.219</b>	<b>6.253</b>	<b>1.159</b>	<b>0.973</b>	<b>0.685</b>

Table 2. Ablation studies on M<sup>3</sup>FD, MEFB and MFIF datasets. The best and second best results are highlighted in **bold**.

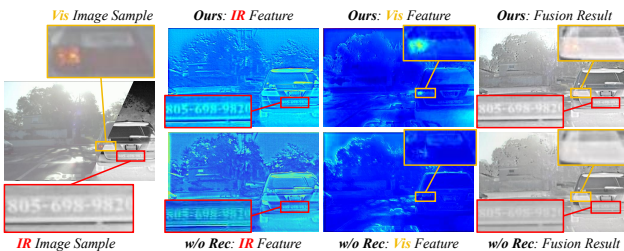


Figure 8. Visualization of encoded features and fusion results with and without the reconstruction alignment module (“Ours” vs “w/o Rec”). The feature maps are extracted from the encoders for the visible and infrared modalities, respectively.

realism of the fused images.

**w/o Reconstruction.** In this configuration, the reconstruction branches for both modalities were removed, and the network was trained solely with the fusion objective. Without reconstruction supervision, the model tended to overfit to shared content and neglect modality-specific information, leading to reduced texture clarity and weaker cross-modality complementarity. This demonstrates that reconstruction plays a crucial role in retaining modality-dependent details and maintaining balanced feature fusion.

To further verify the effectiveness of this module, we visualize the encoded features from the encoders for both the visible and infrared modalities, as well as the final fusion outputs. As shown in Fig. 8, without the reconstruction alignment, the encoded features lose part of their modality-specific semantic representations, such as structural and color-related information. In contrast, our full model (Ours) maintains more faithful modality characteris-

tics in the encoded features, which translates into clearer details and more consistent semantic preservation in the fused results. These results confirm that the reconstruction alignment module effectively regularizes feature learning, encouraging balanced preservation of modality-dependent and shared information, and thus plays a pivotal role in achieving high-quality fusion.

**w/o Bilevel Optimization.** Finally, we removed the bilevel optimization strategy. The performance declined consistently across all datasets, with more pronounced drops in metrics associated with information richness (MI metric) and visual quality (VIF metric). This confirms that bilevel optimization effectively decouples the reconstruction and fusion objectives, stabilizing the training process and enabling more reliable feature disentanglement.

## 5. Conclusion

We propose UniFusion, a unified image fusion framework that achieves superior cross-task generalization while preserving source information fidelity. Unlike existing fusion methods that only focus on combining complementary features, we propose a reconstruction-alignment mechanism that ensures consistent understanding and preservation of source information, allowing modality-specific cues to be retained and aligned throughout the fusion process. Combined with the self-supervised semantic priors of DINOv3, a DINOv3-based feature extractor, and bilevel optimization, it achieves co-adaptation between representation learning and fusion strategy, effectively balancing the trade-off between fusion quality and source information fidelity. Experiments across multi-modal, multi-exposure, and multi-focus tasks show that UniFusion achieves state-of-the-art performance.

## References

- [1] Odysseas Bouzos, Ioannis Andreadis, and Nikolaos Miltioudis. A convolutional neural network-based conditional random field model for structured multi-focus image fusion robust to noise. *IEEE Transactions on Image Processing*, 32: 2915–2930, 2023. 2
- [2] Manisha Das, Deep Gupta, and Ashwini Bakde. An end-to-end content-aware generative adversarial network based method for multimodal medical image fusion. In *Data analytics for intelligent systems: Techniques and solutions*, pages 7–1. IOP Publishing Bristol, UK, 2024. 2
- [3] Songcheng Du, Yang Zou, Zixu Wang, Xingyuan Li, Ying Li, Changjing Shang, and Qiang Shen. Unsupervised hyperspectral image super-resolution via self-supervised modality decoupling. *International Journal of Computer Vision*, 134: 152, 2026. 2
- [4] Zhao Duan, Xiaoliu Luo, and Taiping Zhang. Combining transformers with cnn for multi-focus image fusion. *Expert Systems with Applications*, 235:121156, 2024. 3
- [5] Chengyu Fang, Chunming He, Longxiang Tang, Yuelin Zhang, Chenyang Zhu, Yuqi Shen, Chubin Chen, Guoxia Xu, and Xiu Li. Integrating extra modality helps segmentor find camouflaged objects well. *arXiv preprint arXiv:2502.14471*, 2025. 3
- [6] Chengyu Fang, Heng Guo, Zheng Jiang, Chunming He, Xiu Li, and Minfeng Xu. Photon: Speedup volume understanding with efficient multimodal large language models. In *ICLR*, 2026. 2
- [7] Zijian Gao, Kele Xu, Xingxing Zhang, Huiping Zhuang, Tianjiao Wan, Bo Ding, Xinjun Mao, and Wang Huaimin. Rethinking obscured sub-optimality in analytic learning for exemplar-free class-incremental learning. *IEEE Transactions on Circuits and Systems for Video Technology*, 36(10): 1123–1136, 2025. 5
- [8] Haozhen Gong, Xiaozhong Ji, Yuansen Liu, Wenbin Wu, Xiaoxiao Yan, Jingjing Liu, Kai Wu, Jiazhen Pan, Bailiang Jian, Jiangning Zhang, et al. Med-cmr: A fine-grained benchmark integrating visual evidence and clinical logic for medical complex multimodal reasoning. *arXiv preprint arXiv:2512.00818*, 2025. 2
- [9] Yuanshen Guan, Ruikang Xu, Mingde Yao, Lizhi Wang, and Zhiwei Xiong. Mutual-guided dynamic network for image fusion. In *Proceedings of the 31st ACM international conference on multimedia*, pages 1779–1788, 2023. 5, 6
- [10] Yongxin Guo, Hao Lu, Onur C Koyun, Zhengjie Zhu, Muhammet Fatih Demir, and Metin Nafi Gurcan. Momentum memory for knowledge distillation in computational pathology. *arXiv preprint arXiv:2602.21395*, 2026. 5
- [11] Shantanu Sen Gupta, Shifat Hossain, and Ki-Doo Kim. Hdr-like image from pseudo-exposure image fusion: A genetic algorithm approach. *IEEE Transactions on Consumer Electronics*, 67(2):119–128, 2021. 2
- [12] Zhanbo Huang, Jinyuan Liu, Xin Fan, Risheng Liu, Wei Zhong, and Zhongxuan Luo. Reconet: Recurrent correction network for fast and efficient multi-modality image fusion. In *European conference on computer vision*, pages 539–555. Springer, 2022. 5, 6
- [13] Zefeng Huang, Shen Yang, Jin Wu, Lei Zhu, and Jin Liu. Fusiondiff: A unified image fusion network based on diffusion probabilistic models. *Computer Vision and Image Understanding*, 244:104011, 2024. 2
- [14] Qizhen Lan, Aaron Choi, Jun Ma, Bo Wang, Zhaoming Zhao, Xiaoqian Jiang, and Yu-Chun Hsu. From performance to practice: Knowledge-distilled segmentator for on-premises clinical workflows. *arXiv preprint arXiv:2601.09191*, 2026. 1
- [15] Qizhen Lan, Yu-Chun Hsu, Nida Saddaf Khan, and Xiaoqian Jiang. Reco-kd: Region-and context-aware knowledge distillation for efficient 3d medical image segmentation. *arXiv preprint arXiv:2601.08301*, 2026. 2
- [16] Bingyu Li, Da Zhang, Zhiyuan Zhao, Junyu Gao, and Xuelong Li. Stitchfusion: Weaving any visual modalities to enhance multimodal semantic segmentation. In *Proceedings of the 33rd ACM International Conference on Multimedia*, pages 1308–1317, 2025. 5
- [17] Boyi Li, Yifan Shen, Yuanzhe Liu, Yifan Xu, Jiateng Liu, Xinzhuo Li, Zhengyuan Li, Jingyuan Zhu, Yunhan Zhong, Fangzhou Lan, et al. Toward cognitive supersensing in multimodal large language model. *arXiv preprint arXiv:2602.01541*, 2026. 3
- [18] Hui Li, Tianyang Xu, Xiao-Jun Wu, Jiwen Lu, and Josef Kittler. Lrrnet: A novel representation learning guided fusion network for infrared and visible images. *IEEE transactions on pattern analysis and machine intelligence*, 45(9):11040–11052, 2023. 5, 6
- [19] Huafeng Li, Zengyi Yang, Yafei Zhang, Wei Jia, Zhengtao Yu, and Yu Liu. Mulfs-cap: Multimodal fusion-supervised cross-modality alignment perception for unregistered infrared-visible image fusion. *IEEE Transactions on Pattern Analysis and Machine Intelligence*, 47(5):3673–3690, 2025. 2
- [20] Jiaojiao Li, Songcheng Du, Chaoxiong Wu, Yihong Leng, Rui Song, and Yunsong Li. Dr-cr net: Dense residual channel re-calibration network with non-local purification for spectral super resolution. In *Proceedings of the IEEE/CVF conference on computer vision and pattern recognition*, pages 1259–1268, 2022. 5
- [21] Jiaojiao Li, Songcheng Du, Rui Song, Yunsong Li, and Qian Du. Progressive spatial information-guided deep aggregation convolutional network for hyperspectral spectral super-resolution. *IEEE Transactions on Neural Networks and Learning Systems*, 36(1):1677–1691, 2023. 2
- [22] Xingyuan Li, Yang Zou, Jinyuan Liu, Zhiying Jiang, Long Ma, Xin Fan, and Risheng Liu. From text to pixels: A context-aware semantic synergy solution for infrared and visible image fusion. *arXiv preprint arXiv:2401.00421*, 2023. 3
- [23] Xingyuan Li, Jinyuan Liu, Zhixin Chen, Yang Zou, Long Ma, Xin Fan, and Risheng Liu. Contourlet residual for prompt learning enhanced infrared image super-resolution. In *European Conference on Computer Vision*, pages 270–288. Springer, 2024. 2

- [24] Xingyuan Li, Zirui Wang, Yang Zou, Zhixin Chen, Jun Ma, Zhiying Jiang, Long Ma, and Jinyuan Liu. Difisir: A diffusion model with gradient guidance for infrared image super-resolution. In *Proceedings of the Computer Vision and Pattern Recognition Conference*, pages 7534–7544, 2025. 2
- [25] Yuqi Li, Junhao Dong, Chuanguang Yang, Shiping Wen, Piotr Koniusz, Tingwen Huang, Yingli Tian, and Yew-Soon Ong. Mmt-ard: Multimodal multi-teacher adversarial distillation for robust vision-language models. *arXiv preprint arXiv:2511.17448*, 2025. 3
- [26] Nannan Liang. Medical image fusion with deep neural networks. *Scientific Reports*, 14(1):7972, 2024. 2
- [27] Pengwei Liang, Junjun Jiang, Xianming Liu, and Jiayi Ma. Fusion from decomposition: A self-supervised decomposition approach for image fusion. In *European conference on computer vision*, pages 719–735. Springer, 2022. 5, 6
- [28] Jinyuan Liu, Xin Fan, Zhanbo Huang, Guanyao Wu, Risheng Liu, Wei Zhong, and Zhongxuan Luo. Target-aware dual adversarial learning and a multi-scenario multi-modality benchmark to fuse infrared and visible for object detection. In *Proceedings of the IEEE/CVF conference on computer vision and pattern recognition*, pages 5802–5811, 2022. 2, 5
- [29] Jinyuan Liu, Zhu Liu, Guanyao Wu, Long Ma, Risheng Liu, Wei Zhong, Zhongxuan Luo, and Xin Fan. Multi-interactive feature learning and a full-time multi-modality benchmark for image fusion and segmentation. In *Proceedings of the IEEE/CVF international conference on computer vision*, pages 8115–8124, 2023. 1
- [30] Jinyuan Liu, Xingyuan Li, Zirui Wang, Zhiying Jiang, Wei Zhong, Wei Fan, and Bin Xu. Promptfusion: Harmonized semantic prompt learning for infrared and visible image fusion. *IEEE/CAA Journal of Automatica Sinica*, 2024. 2
- [31] Jinyuan Liu, Runjia Lin, Guanyao Wu, Risheng Liu, Zhongxuan Luo, and Xin Fan. Coconet: Coupled contrastive learning network with multi-level feature ensemble for multi-modality image fusion. *International Journal of Computer Vision*, 132(5):1748–1775, 2024. 1, 5, 6
- [32] Jinyuan Liu, Bowei Zhang, Qingyun Mei, Xingyuan Li, Yang Zou, Zhiying Jiang, Long Ma, Risheng Liu, and Xin Fan. Dcevo: Discriminative cross-dimensional evolutionary learning for infrared and visible image fusion. In *Proceedings of the IEEE/CVF Conference on Computer Vision and Pattern Recognition*, pages 2226–2235, 2025. 2
- [33] Yu Liu, Xun Chen, Rabab K Ward, and Z Jane Wang. Image fusion with convolutional sparse representation. *IEEE signal processing letters*, 23(12):1882–1886, 2016. 3
- [34] Jiayi Ma, Linfeng Tang, Fan Fan, Jun Huang, Xiaoguang Mei, and Yong Ma. Swinfusion: Cross-domain long-range learning for general image fusion via swin transformer. *IEEE/CAA Journal of Automatica Sinica*, 9(7):1200–1217, 2022. 2, 3, 5, 6
- [35] Yue Ma, Kunyu Feng, Zhongyuan Hu, Xinyu Wang, Yucheng Wang, Mingzhe Zheng, Xuanhua He, Chenyang Zhu, Hongyu Liu, Yingqing He, et al. Controllable video generation: A survey. *arXiv preprint arXiv:2507.16869*, 2025. 2
- [36] Yue Ma, Yingqing He, Hongfa Wang, Andong Wang, Leqi Shen, Chenyang Qi, Jixuan Ying, Chengfei Cai, Zhifeng Li, Heung-Yeung Shum, et al. Follow-your-click: Open-domain regional image animation via motion prompts. In *Proceedings of the AAAI Conference on Artificial Intelligence*, pages 6018–6026, 2025. 3
- [37] Yue Ma, Zhikai Wang, Tianhao Ren, Mingzhe Zheng, Hongyu Liu, Jiayi Guo, Mark Fong, Yuxuan Xue, Zixiang Zhao, Konrad Schindler, et al. Fastvmt: Eliminating redundancy in video motion transfer. *arXiv preprint arXiv:2602.05551*, 2026. 2
- [38] Mansour Nejati, Shadrokh Samavi, and Shahram Shirani. Multi-focus image fusion using dictionary-based sparse representation. *Information fusion*, 25:72–84, 2015. 5
- [39] Yuncan Ouyang, Hao Zhai, Hanyue Hu, Xiaohang Li, and Zhi Zeng. Fusiongc: Multi-focus image fusion using superpixel features generation gc and pixel-level feature reconstruction cnn. *Expert Systems with Applications*, 262: 125665, 2025. 2
- [40] Mojtaba Safari, Ali Fatemi, and Louis Archambault. Medfusiongan: multimodal medical image fusion using an unsupervised deep generative adversarial network. *BMC Medical Imaging*, 23(1):203, 2023. 2
- [41] Jiang Shao, Xinbo Zhao, Xiaochun Zou, and Xiaolin Ye. Egohiermask: Hierarchical semantic-prior guided masked autoencoder for egocentric action recognition. In *Proceedings of the 33rd ACM International Conference on Multimedia*, pages 8711–8720, 2025. 5
- [42] Yifan Shen, Yuanzhe Liu, Jinyuan Zhu, Xu Cao, Xiaofeng Zhang, Yixiao He, Wenming Ye, James Matthew Rehg, and Ismini Lourentzou. Fine-grained preference optimization improves spatial reasoning in vlms. *arXiv preprint arXiv:2506.21656*, 2025. 3
- [43] Yu Shi, Yu Liu, Juan Cheng, Z Jane Wang, and Xun Chen. Vdmufusion: A versatile diffusion model-based unsupervised framework for image fusion. *IEEE Transactions on Image Processing*, 34:441–454, 2024. 3
- [44] Oriane Siméoni, Huy V Vo, Maximilian Seitzer, Federico Baldassarre, Maxime Oquab, Cijo Jose, Vasil Khalidov, Marc Szafraniec, Seungeun Yi, Michaël Ramamonjisoa, et al. Dinov3. *arXiv preprint arXiv:2508.10104*, 2025. 2
- [45] Wei Tang and Fazhi He. Fatfusion: A functional–anatomical transformer for medical image fusion. *Information Processing & Management*, 61(4):103687, 2024. 2
- [46] Alexander Toet and Maarten A Hogervorst. Progress in color night vision. *Optical Engineering*, 51(1):010901–010901, 2012. 5
- [47] Di Wang, Jinyuan Liu, Xin Fan, and Risheng Liu. Unsupervised misaligned infrared and visible image fusion via cross-modality image generation and registration. *arXiv preprint arXiv:2205.11876*, 2022. 2, 5, 6
- [48] Zirui Wang, Jiayi Zhang, Tianwei Guan, Yuhan Zhou, Xingyuan Li, Minjing Dong, and Jinyuan Liu. Efficient rectified flow for image fusion. In *The Thirty-ninth Annual Conference on Neural Information Processing Systems*, 2025. 3
- [49] Yanbin Wei, Jiangyue Yan, Chun Kang, Yang Chen, Hua Liu, James Kwok, and Yu Zhang. Dynamicgtr: Leveraging graph topology representation preferences to boost vlm capabilities on graph qas. *arXiv preprint arXiv:2602.21864*, 2026. 3

- [50] Bin Xiao, Haifeng Wu, and Xiuli Bi. Dtmnet: A discrete tchebichef moments-based deep neural network for multi-focus image fusion. In *Proceedings of the IEEE/CVF International Conference on Computer Vision*, pages 43–51, 2021. 2
- [51] Han Xu, Jiayi Ma, Junjun Jiang, Xiaojie Guo, and Haibin Ling. U2fusion: A unified unsupervised image fusion network. *IEEE transactions on pattern analysis and machine intelligence*, 44(1):502–518, 2020. 2, 3, 5, 6
- [52] Han Xu, Jiayi Ma, Zhuliang Le, Junjun Jiang, and Xiaojie Guo. Fusiondn: A unified densely connected network for image fusion. In *Proceedings of the AAAI conference on artificial intelligence*, pages 12484–12491, 2020. 5
- [53] Han Xu, Jiayi Ma, and Xiao-Ping Zhang. Mef-gan: Multi-exposure image fusion via generative adversarial networks. *IEEE Transactions on Image Processing*, 29:7203–7216, 2020. 2
- [54] Jiyang Xu, Qi Wang, Xin Xiong, Di Gai, Ruihua Zhou, and Dong Wang. Clip-driven view-aware prompt learning for unsupervised vehicle re-identification. In *Proceedings of the AAAI Conference on Artificial Intelligence*, pages 8896–8904, 2025. 3
- [55] Shuang Xu, Xiaoli Wei, Chunxia Zhang, Junmin Liu, and Jianshe Zhang. Mffw: A new dataset for multi-focus image fusion. *arXiv preprint arXiv:2002.04780*, 2020. 5
- [56] Zengyi Yang, Yafei Zhang, Huaifeng Li, and Yu Liu. Instruction-driven fusion of infrared-visible images: Tailoring for diverse downstream tasks. *Information Fusion*, 121: 103148, 2025. 2
- [57] Xunpeng Yi, Han Xu, Hao Zhang, Linfeng Tang, and Jiayi Ma. Text-if: Leveraging semantic text guidance for degradation-aware and interactive image fusion. In *Proceedings of the IEEE/CVF Conference on Computer Vision and Pattern Recognition*, pages 27026–27035, 2024. 1, 2, 3
- [58] Hao Zhang, Zhuliang Le, Zhenfeng Shao, Han Xu, and Jiayi Ma. Mff-gan: An unsupervised generative adversarial network with adaptive and gradient joint constraints for multi-focus image fusion. *Information Fusion*, 66:40–53, 2021. 2, 5
- [59] Xingchen Zhang. Benchmarking and comparing multi-exposure image fusion algorithms. *Information Fusion*, 74: 111–131, 2021. 5
- [60] Xingchen Zhang. Deep learning-based multi-focus image fusion: A survey and a comparative study. *IEEE Transactions on Pattern Analysis and Machine Intelligence*, 44(9): 4819–4838, 2021. 5
- [61] Wenda Zhao, Shigeng Xie, Fan Zhao, You He, and Huchuan Lu. Metafusion: Infrared and visible image fusion via meta-feature embedding from object detection. In *Proceedings of the IEEE/CVF Conference on Computer Vision and Pattern Recognition*, pages 13955–13965, 2023. 2
- [62] Zixiang Zhao, Shuang Xu, Chunxia Zhang, Junmin Liu, Pengfei Li, and Jianshe Zhang. Didfuse: Deep image decomposition for infrared and visible image fusion. *arXiv preprint arXiv:2003.09210*, 2020. 2
- [63] Zixiang Zhao, Jianshe Zhang, Shuang Xu, Zudi Lin, and Hanspeter Pfister. Discrete cosine transform network for guided depth map super-resolution. In *Proceedings of the IEEE/CVF conference on computer vision and pattern recognition*, pages 5697–5707, 2022. 2
- [64] Zixiang Zhao, Haowen Bai, Jianshe Zhang, Yulun Zhang, Shuang Xu, Zudi Lin, Radu Timofte, and Luc Van Gool. Cddfuse: Correlation-driven dual-branch feature decomposition for multi-modality image fusion. In *Proceedings of the IEEE/CVF conference on computer vision and pattern recognition*, pages 5906–5916, 2023. 1, 2, 5, 6
- [65] Zixiang Zhao, Haowen Bai, Yuanzhi Zhu, Jianshe Zhang, Shuang Xu, Yulun Zhang, Kai Zhang, Deyu Meng, Radu Timofte, and Luc Van Gool. Ddfm: denoising diffusion model for multi-modality image fusion. In *Proceedings of the IEEE/CVF international conference on computer vision*, pages 8082–8093, 2023. 2
- [66] Zixiang Zhao, Jianshe Zhang, Xiang Gu, Chengli Tan, Shuang Xu, Yulun Zhang, Radu Timofte, and Luc Van Gool. Spherical space feature decomposition for guided depth map super-resolution. In *Proceedings of the IEEE/CVF International Conference on Computer Vision*, pages 12547–12558, 2023. 2
- [67] Zixiang Zhao, Haowen Bai, Jianshe Zhang, Yulun Zhang, Kai Zhang, Shuang Xu, Dongdong Chen, Radu Timofte, and Luc Van Gool. Equivariant multi-modality image fusion. In *Proceedings of the IEEE/CVF conference on computer vision and pattern recognition*, pages 25912–25921, 2024. 3
- [68] Man Zhou, Jie Huang, Keyu Yan, Danfeng Hong, Xiuping Jia, Jocelyn Chanussot, and Chongyi Li. A general spatial-frequency learning framework for multimodal image fusion. *IEEE Transactions on Pattern Analysis and Machine Intelligence*, 2024. 2
- [69] Pengfei Zhu, Yang Sun, Bing Cao, and Qinghua Hu. Task-customized mixture of adapters for general image fusion. In *Proceedings of the IEEE/CVF conference on computer vision and pattern recognition*, pages 7099–7108, 2024. 3, 5, 6
- [70] Yang Zou, Zhixin Chen, Zhipeng Zhang, Xingyuan Li, Long Ma, Jinyuan Liu, Peng Wang, and Yanning Zhang. Contourlet refinement gate framework for thermal spectrum distribution regularized infrared image super-resolution. *International Journal of Computer Vision*, 134(1):23, 2026. 2
- [71] Yang Zou, Jun Ma, Zhidong Jiao, Xingyuan Li, Zhiying Jiang, and Jinyuan Liu. Toward real-world infrared image super-resolution: A unified autoregressive framework and benchmark dataset. *arXiv preprint arXiv:2603.04745*, 2026. 1